

Evidence for Bose-Einstein Condensation of a Two-Component Exciton Gas

D. W. Snoke and J. P. Wolfe

*Physics Department and Materials Research Laboratory, University of Illinois at Urbana-Champaign,
1110 West Green Street, Urbana, Illinois 61801*

A. Mysyrowicz

*Laboratoire d'Optique Appliquée, Ecole Nationale Supérieure de Techniques Avancées,
Ecole Polytechnique, Palaiseau F-91120, France
and Groupe de Physique des Solides, Université de Paris 7, Paris, France*

(Received 7 March 1990)

Time-resolved spectral and spatial measurements of photoluminescence in Cu_2O at low temperatures suggest that the gas of paraexcitons undergoes Bose-Einstein condensation at high densities. As a result of the two-component nature of the gas (orthoexcitons and paraexcitons with different ground-state energies and spin multiplicities) and the nonequilibrium nature of photoproduced excitons, the condensation process is quite different from the simple ideal-gas case envisioned by Einstein.

PACS numbers: 71.35.+z, 05.30.Jp, 67.90.+z, 78.55.Hx

It is well known that the Maxwell-Boltzmann formula describing the kinetic-energy distribution of atoms in a gas is only an approximation. At low temperatures or high densities, the true quantum nature of the particles becomes manifest, and the correct distribution function depends on the spin quantum number associated with the particles. For half-integer spin value (Fermi-Dirac statistics), the Pauli exclusion principle prevents multiple occupancy of available quantum states, so that the gas retains kinetic energy even in the limit of zero temperature. Conversely, there is a tendency for integer-spin particles to pile up in states which are already occupied. According to Einstein, in equilibrium this should lead to a phase transition at finite temperatures in which all particles in excess of a critical number go into the lowest quantum state. In the case of an ideal noninteracting gas, the critical density for Bose-Einstein condensation (BEC) is given by $n_c(T) = gCT^{3/2}$, where g is the spin multiplicity and C is a constant depending on the particle mass and universal constants.

Fermi-Dirac statistics are observed in many systems, for instance, in the free-electron gas of metals or in the electron-hole liquid of excited semiconductors. In contrast, the only experimental evidence for Bose-Einstein statistics is provided by liquid helium and excitonic particles in semiconductors.¹⁻⁴

In this Letter, we report evidence for BEC of paraexcitons in Cu_2O ; however, the observations are not as simply described as in the ideal case considered by Einstein. The interesting complication is that the exciton gas has two well-resolved components—orthoexcitons and paraexcitons—which coexist in the same effective volume with different densities. Basically, we have succeeded in producing the paraexciton component at densities above n_c , and under these conditions the exciton gas exhibits unusual spectral and spatial properties which suggest a condensed phase exhibiting rapid transport.

The experimental evidence relies upon time- and space-resolved spectral analysis of the exciton lumines-

cence following optical creation of free-electron-hole pairs. In the experiments, a high-purity Cu_2O sample is excited with the green light from an Ar^{2+} -ion laser ($h\nu = 2.42$ eV) operating in the cavity-dumped mode (pulse duration ≈ 10 ns). The strong optical absorption ($a = 6000$ cm^{-1}) produces an initially excited crystal volume in the form of a flat pancake of depth a^{-1} and lateral dimensions between 10 μm and 2 mm, depending on the laser focusing. The incident pulse power of about 50 W therefore results in a generation rate of up to 10^{21} $\text{ns}^{-1}\text{cm}^{-3}$.

Following optical injection of free-electron-hole pairs, exciton formation and relaxation to the bottom of the $n=1$ kinetic-energy band proceeds in a time scale of the order 10^{-12} s. Electron-hole exchange interaction splits the $n=1$ excitons into triplet orthoexcitons and singlet paraexcitons, with the para state lying 12 meV lower in energy. The initial population ratio of orthoexcitons to paraexcitons is expected to be equal to the 3:1 ratio of their spin multiplicities.

In previous experiments,^{2,4} which concentrated on the orthoexciton luminescence due to its much higher radiative efficiency, it was shown that the orthoexciton energy distribution evolves continuously, from a classical regime at low densities to a highly quantum-degenerate one, with an associated internal chemical potential, $\mu \approx 0$, in excellent agreement with the predictions of the ideal-Bose-gas model. The distribution function can be inferred directly from the line shape of the phonon-assisted recombination luminescence of orthoexcitons. The value $\mu \approx 0$ means that the conditions for BEC of orthoexcitons are approached very closely.

Under such conditions, it becomes interesting to examine the properties of paraexcitons also present, especially in view of the facts that (a) the critical density for BEC is smaller than that of orthoexcitons by a factor $g=3$, and (b) the paraexciton density is increased by down-conversion of orthoexcitons.⁵ This raises the possibility that BEC of paraexcitons is actually achieved when

$\mu \approx 0$ for orthoexcitons.

Despite the difficulty that the paraexciton radiative efficiency is over 10^3 times smaller than that of the orthoexcitons, we have been able to observe its Γ_5^- phonon-assisted recombination luminescence by long averaging with time-resolved photon counting. Figure 1 shows the simultaneous kinetic-energy distributions for orthoexcitons and paraexcitons at the peak of a laser pulse focused to a medium power density of about 5×10^6 W/cm².

The notable difference between these two spectra is that the paraexciton distribution is sharper. This is easily seen from the dotted lines which mark the spectral half-widths. The narrower spectrum implies that the paraexcitons are more degenerate than the orthoexcitons, i.e., closer to condensation. This conclusion is based on the assumption that the temperatures of the para and ortho components are nearly the same. Certainly the rapid scattering rate between particles, about 10^{11} s⁻¹ at a density of 10^{18} cm⁻³, supports this hypothesis, assuming that the two gas components occupy the same volume. Figure 3, discussed below, indicates that this is indeed the case. We now examine the spectra more quantitatively.

Determination of paraexciton density.—Once a ho-

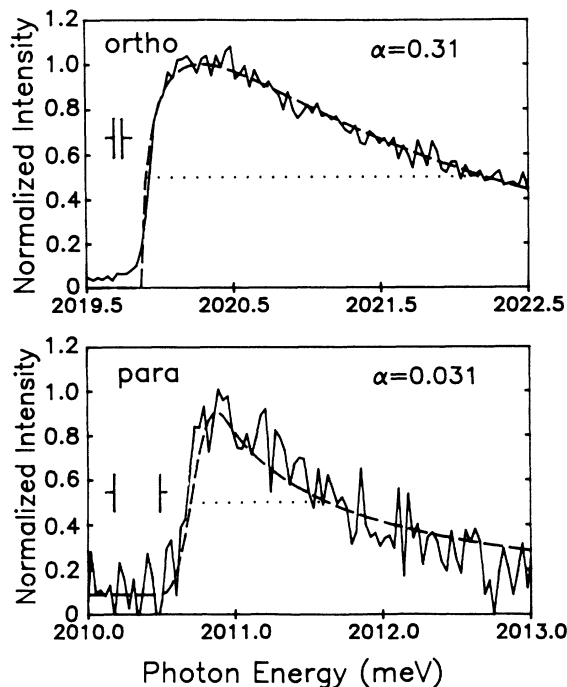


FIG. 1. Simultaneous orthoexciton (Γ_3^- phonon replica) and paraexciton (Γ_5^- replica) spectra at the peak of a laser pulse with incident power $\approx 5 \times 10^6$ W/cm². A base line has been subtracted from the paraexciton spectrum. The half-widths are shown by the dotted lines. The paraexciton luminescence has a much smaller half-width, indicating that they are more degenerate than the orthoexcitons. Both spectra are fitted with a BE distribution with $T=25$ K and the given α .

mogeneous gas enters the quantum regime $|\mu/k_B T| \leq 1$, an absolute calibration of its density is provided by the relation

$$n(\alpha, T) = g \left(\frac{m}{2\pi\hbar^2} \right)^{3/2} (k_B T)^{3/2} \int f(\epsilon, \alpha) \epsilon^{1/2} d\epsilon, \quad (1)$$

where $m = 2.7m_0$ is the exciton mass,⁶ $f(\epsilon, \alpha) = 1/[\exp(\epsilon + \alpha) - 1]$ is the Bose-Einstein distribution function with $\epsilon \equiv E/k_B T$ and $\alpha \equiv -\mu/k_B T$. Fitting the shapes of the phonon-assisted recombination lines of the excitons by the kinetic-energy distribution $\epsilon^{1/2} f(\epsilon, \alpha)$ gives values for α and T , as shown for the orthoexcitons in Fig. 1. In this medium-power case, Eq. (1) yields $n(\text{ortho}) = 0.5n_c(\text{ortho})$. We find that this conclusion is not significantly affected by gas inhomogeneities.⁷ Under the previously discussed assumption that the orthoexcitons and paraexcitons have the same temperature, a fit of the paraexciton spectrum yields $\alpha = 0.03$, corresponding to $n(\text{para}) = 0.8n_c(\text{para})$ at this excitation level.

An independent measure of the paraexciton density is obtained from the ratio of (spectrally integrated) intensities of the two luminescence lines. This method relies on a previous calibration⁸ of the ortho and para radiative strengths for Γ_5^- phonon-assisted emission (a factor of 50), and our observation that the Γ_3^- and Γ_5^- orthoexciton replicas have a relative strength of 30 ± 5 . Therefore, for the same number of particles, the Γ_5^- para spectrum should be $50 \times 30 = 1500 \pm 400$ times weaker than the ortho spectrum.⁹ Taking $n(\text{ortho}) = 3.5 \times 10^{18}$ cm⁻³ from the fit in Fig. 1 and the relative integrated intensities of these two spectra, we find $n(\text{para}) = 2.8 \times 10^{18}$ cm⁻³, which is about 50% above its critical density at the assumed temperature. Clearly, the paraexciton gas is highly degenerate. The factor-of-2 discrepancy in the two methods of determining the gas density may be due to uncertainties in the analyses or due to interactions that modify the ideal-gas distributions.

At this point, it is important to realize that an ideal gas with a significant condensed fraction at $k=0$ should not exhibit a two-peaked structure—one peak due to a $k=0$ spike and one due to the excited-state spectrum—as is frequently assumed. For $\mu=0$, the $f(\epsilon)$ distribution function of excited particles is strongly peaked at $\epsilon=0$. Collisional broadening and finite spectrometer resolution must be properly accounted for in order to extract the condensed fraction of the gas from the spectrum.

Anomalous paraexciton luminescence.—How do the orthoexciton and paraexciton energy distributions depend on excitation power? Excitation densities of up to 2×10^7 W/cm² are obtained by decreasing the laser spot size to about $10 \mu\text{m}$ at constant power. Figure 2(a) shows the orthoexciton spectra at three excitation densities. As previously observed,⁴ both the density and temperature of the orthoexciton gas increase with power, and the chemical potential “saturates” at a value near $-0.1k_B T$, implying $n(\text{ortho}) \approx 0.6n_c(\text{ortho})$. At this

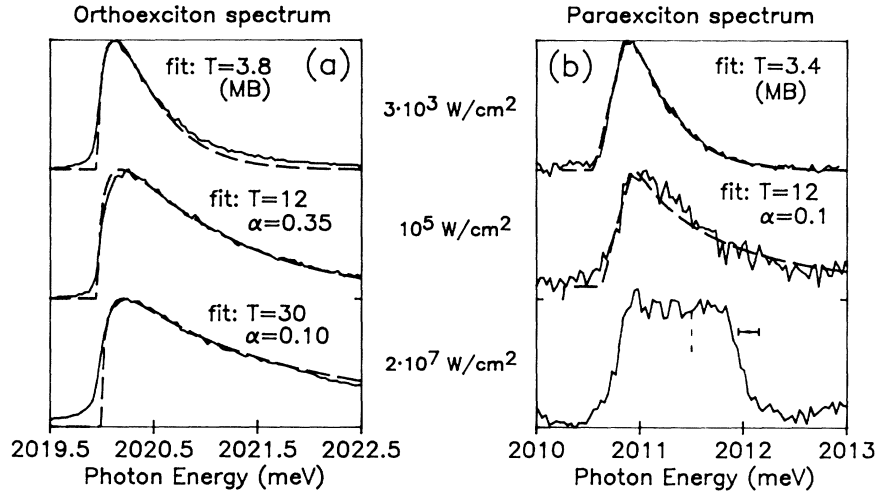


FIG. 2. Simultaneous orthoexciton and paraexciton spectra at the peak of the laser pulse for the three incident powers shown. A base line has been subtracted from each of the lower two paraexciton spectra. The paraexciton spectrum at high density takes on an anomalous shape. The dashed line on this spectrum indicates the energy of an exciton which couples directly to the ground state via a longitudinal-acoustic phonon (see text). The solid bar indicates the energy of a paraexciton created by an orthoexciton in the $k=0$ state emitting a 10.9-meV optical phonon and converting to a paraexciton.

highest excitation level, the ratio of integrated intensities implies that the paraexciton density exceeds $n_c(\text{para})$ by nearly a factor of 5.

As shown in Fig. 2(b), the paraexciton spectrum at these supercritical densities is highly anomalous. A “bump,” or steplike high-energy edge, appears at about 1 meV above the paraexciton ground state. This feature appears for a period of about 10 ns during the pulse and no anomalies are simultaneously observed for the orthoexcitons. During this period the spectral position of the bump remains at the same energy position.

These data suggest that BEC is occurring in a state of nonzero momentum. But why the fixed energy at about 1 meV? We suggest that the lattice phonons are playing an important role in this novel behavior. Two possibilities come to mind:

(a) The linear dispersion of the longitudinal-acoustic phonons in Cu_2O , $\hbar\omega = \hbar vk$ with $v = 4.5 \times 10^5$ cm/s, crosses the quadratic dispersion of excitons at an energy of about 0.7 meV, shown as the dashed line in Fig. 2(b). Nonequilibrium phonons flowing from the excitation spot can impart their momentum to the gas, which, if superfluid, would take on a rapid ballistic transport.

(b) The degenerate orthoexcitons may be “seeding” the paraexciton distribution at finite energy, producing a condensate of nonzero momentum. Ortho-to-para conversion with the emission of a single Γ_5^- optical phonon would occur at an energy with experimental uncertainty indicated by the bar in Fig. 2(b), assuming an orthoexciton with $k=0$.

Thus the lattice phonons provide two intrinsic energies which are close to that of the observed paraexciton bump.¹⁰

Anomalous exciton transport.—The possibility of

superfluid transport of the excitons has prompted us to examine the spatial distribution of the gas. Time-resolved spatial profiles are obtained by scanning a magnified image of the sample across the entrance slit of the spectrometer, while photon counting with a selected time gate. Spectral selection of about 1 meV is chosen by an appropriate exit slit of the spectrometer. The results are shown in Fig. 3(a).

The solid curves in this figure are obtained with spectral selection at the orthoexciton Γ_3^- luminescence, and the solid curves select the Γ_5^- paraexciton line. Both components of the exciton gas are seen to expand into the crystal; in fact, their motion is nearly identical.

The expansion rate of the exciton gas is found to be dependent on excitation density, as shown in Fig. 3(b). At the lowest levels, the expansion is comparable to the previously measured¹¹ diffusive behavior of paraexcitons, for which $D = 600$ cm²/s at a temperature of 4 K. However, at high excitation a ballisticlike or drift behavior is observed in the present data, and the velocity actually exceeds the longitudinal sound velocity in Cu_2O . The fastest expansion rate, 0.65×10^6 cm/s, is comparable to the ballistic velocity, 1.1×10^6 cm/s, of an exciton with 1-meV kinetic energy, which corresponds the bump in the paraexciton spectrum.

Discussion of results.—These experiments show that BEC of an excitonic gas intimately involves the coupled dynamics of both ortho and para components. Do the striking spectral and spatial results imply a superfluid flow of Bose-condensed excitons? Further intriguing observations and issues bear on the answer to this question:

(a) The ballisticlike transport extends well beyond the 10-ns laser pulse and long after the paraexciton bump has disappeared. The gas is cooling continuously during

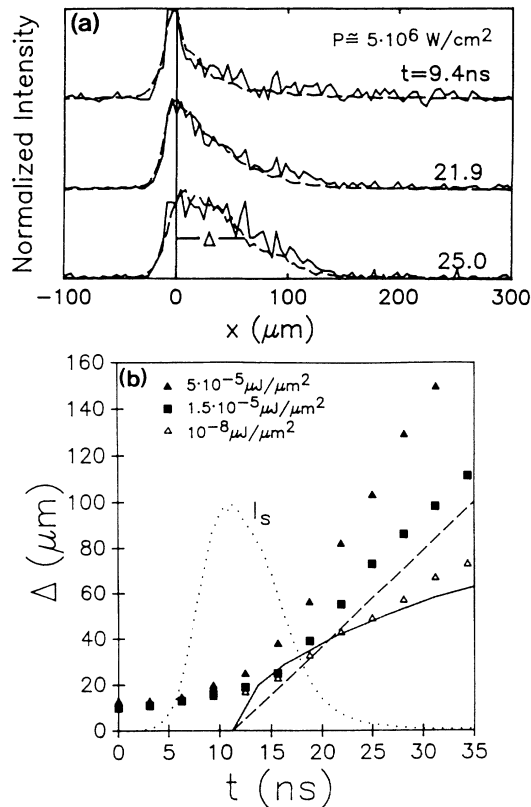


FIG. 3. (a) Solid curves: The normalized paraexciton spatial distribution for three times during and after the laser pulse. The early-time paraexciton, remaining from the previous laser pulse, has been subtracted. $x=0$ corresponds to the crystal surface. Dashed curves: the orthoexciton distribution normalized to the same height. (b) *Supersonic transport of excitons at high power*. Time-resolved width of orthoexciton profile for several excitation densities. Δ is defined in (a). The dashed line has a slope given by the average longitudinal-acoustic phonon velocity in Cu_2O , 4.5×10^5 cm/s. The solid curve equals $[2.77D(t-t_0)]^{1/2}$, with $D=600$ cm^2/s , previously measured (Ref. 11) for paraexcitons at $T=2$ K. The dotted line labeled I_s gives the total luminescence at the surface of the crystal as a function of time, which roughly follows the laser intensity.

this rapid transport and remains degenerate ($\alpha \leq 0.2$) for at least 10 ns beyond the peak of the pulse.⁴

(b) Both orthoexciton and paraexciton spatial profiles show rapid transport, although the orthoexcitons are much less degenerate than the paraexcitons. The correlation of orthoexciton and paraexciton expansion may indicate a dragging of the orthoexcitons by superfluid paraexcitons. Another possibility is that the orthoexcitons are produced by the paraexcitons deep in the crystal, possibly through an Auger process.¹²

(c) The spatial distribution of the exciton gas may be affected by particle lifetimes, which decrease with increasing density due to two-body (e.g., Auger) recombination. This would tend to reduce the high-density regions faster than the low-density regions, apparently speeding up the expansion rate. Also, the gas temperatures are much higher at high density, possibly leading to

a density dependence of the diffusion constant. It is unlikely, however, that these effects could account for the nearly ballistic transport velocities which we observe.

(d) Our spectral analysis so far has assumed a weakly interacting gas, based on the agreement between ideal-gas distributions and the observed spectra, and because $na_x^3=0.01$ for an exciton radius of $a_x=7$ Å and a gas density of $n=3 \times 10^{19}$ cm^{-3} . Interactions, which are a prerequisite for superfluidity, produce a broadening of the energy distribution. In liquid helium, for example, the particle momenta exhibit a 15-K near Maxwellian distribution even well below the superfluid transition temperature of 2.17 K. Also, the low-energy excitations of a superfluid have a phononlike dispersion that may affect the excitonic energy distribution and transport.

This work is supported by the National Science Foundation, Grant No. DMR87-22761. Facility support is provided by the NSF under the Materials Research Laboratory Grant No. DMR86-12860. Natural Cu_2O samples were obtained by a gift from P. J. Dunn of the Smithsonian Institute. We benefited from several discussions with A. Griffin and P. Nozières. Laboratoire d'Optique Appliquée, Ecole Nationale Supérieure de Techniques Avancées, and Groupe de Physique des Solides are laboratoires Associés au CNRS.

¹See reviews by E. Hanamura and H. Haug, Phys. Rep. **33**, 209 (1977); C. Comte and P. Nozières, J. Phys. (Paris) **43**, 1069 (1982); A. Mysyrowicz, J. Phys. (Paris) **41**, Suppl. 7, 281 (1980).

²D. Hulin, A. Mysyrowicz, and C. Benoît à la Guillaume, Phys. Rev. Lett. **45**, 1970 (1980).

³N. Peghambarian, L. L. Chase, and A. Mysyrowicz, Phys. Rev. B **27**, 2325 (1983).

⁴D. Snoke, J. P. Wolfe, and A. Mysyrowicz, Phys. Rev. Lett. **59**, 827 (1987).

⁵D. W. Snoke, D. P. Trauernicht, and J. P. Wolfe, Phys. Rev. B **41**, 5266 (1990).

⁶N. Caswell, J. S. Weiner, and P. Y. Yu, Solid State Commun. **40**, 843 (1981).

⁷D. W. Snoke, J. P. Wolfe, and A. Mysyrowicz, Phys. Rev. B (to be published).

⁸P. D. Bloch and C. Schwab, Phys. Rev. Lett. **41**, 514 (1978).

⁹This factor of 1500 is close to the factor of 2000 determined by A. Mysyrowicz, D. Hulin, and A. Antonetti, Phys. Rev. Lett. **43**, 1123 (1979); **43**, 1275(E) (1979). Note that $\Gamma_{12} = \Gamma_3, \Gamma_{25} = \Gamma_5$.

¹⁰Another interpretation is suggested by Moskalkenko's prediction that the condensed paraexciton gas will exhibit a density-dependent blueshift; see S. A. Moskalkenko, A. I. Bobrysheva, S. S. Russu, V. V. Balgata, and A. V. Lelyakov, J. Phys. (Paris) **18**, 1989 (1985). However, the paraexciton bump appears not to shift significantly with density.

¹¹D. P. Trauernicht, J. P. Wolfe, and A. Mysyrowicz, Phys. Rev. Lett. **52**, 855 (1984); D. P. Trauernicht and J. P. Wolfe, Phys. Rev. B **33**, 8506 (1986).

¹²A. Mysyrowicz, D. Hulin, and C. Benoît à la Guillaume, J. Lumin. **24/25**, 629 (1981); D. P. Trauernicht, J. P. Wolfe, and A. Mysyrowicz, Phys. Rev. B **34**, 2561 (1986).